Numerical MicroLocal Analysis of 2-D Noisy Harmonic Plane and Circular Waves

J-D, Benamou[1] and F. Collino[2] S. Marmorat[1]

[1] INRIA, Domaine de Voluceau, Rocquencourt, France,
[2] CERFACS, 42 avenue G. Coriolis 31057, Toulouse, France,

E-mail: `Jean-david.Benamou@inria.fr`

Abstract. We present a mathematical and numerical analysis of the stability and accuracy of the `NMLA` (Numerical MicroLocal Analysis) method [2] and its discretization. We restrict to homogeneous space and focus on the two simplest cases : 1) Noisy plane wave packets, 2) Noisy point source solutions. A stability result is obtained through the introduction of a new "impedance" observable. The analysis of the point source case leads to a modified second order (curvature dependent) correction of the algorithm. Since `NMLA` is local, this second order improved version can be applied to general data (heterogeneous media). See [1] for a an application to a source discovery inverse problem.

Keywords :plane waves, point source, inverse scattering

AMS classification scheme numbers: 78A05, 78A46, 78M35

1. Introduction

The use of a *formal high frequency asymptotic solution*‡ of the Helmholtz equation can be traced back to a 1911 paper of Debye on "the article of Sommerfeld", see [11]. It marked the beginning of the development of modern Geometric Optics (GO) numerical models and methods for the simulation of high frequency wave propagation which have been used in industry for decades, see [4] [7] for instance. Geometric optics phase and amplitudes are computed either analytically or using frequency independent PDE's and then used to reconstruct high frequency asymptotic approximation of waves.

In [2], we tried to address the problem of numerically and locally extracting the GO components from harmonic wavefields. This difficult non linear inverse problem is usually reduced trough linearization to a plane wave packet approximation, an approach classically followed in signal processing for Direction of Arrival analysis for instance (`MUSIC, ESPRIT` [14]) or "events" analysis in Image Processing (Plane Wave Destructor [12], Radon transform [3]). We also used the linearized plane wave model and proposed an algorithm named `NMLA` for *Numerical MicroLocal Analysis* to solve this problem. It is based on a family of linear operators (or filters) B_k, indexed by the wavenumber k, see (4) below. The filters are applied to observed harmonic wave data u_k collected on a circle

‡ also known as an Ansatz.

of fixed radius r_0 around an observation point x_0. They simply consist in weighting the Fourier modes of the (periodic) observable. The first version of `NMLA` used Dirichlet data,

$$U_k(\hat{s}) = u_k(x), \quad x = x_0 + r_0\hat{s}, \quad \hat{s} = (\cos\theta, \sin\theta). \tag{1}$$

When B_k is applied to an observable constructed from a finite number of plane waves,

$$u_k(x) = \sum_{p=1}^{P} b_p e^{-ik(x-x_0)\cdot\hat{s}_p}, \tag{2}$$

the output is an angular function $(B_k U_k) : \theta \in [0, 2\pi[\to \mathbb{C}$ whose P largest maxima of amplitude b_p approximately localize the angles θ_p of the directions $\hat{s}_p$'s. Both the localization of the peaks and the quality of the evaluation of the amplitudes b_p increase with the frequency as we move into the high frequency asymptotic regime, thus allowing in principle to estimate the number of high frequency wavefronts passing through x_0, their directions and amplitudes.

The specific circle geometry has advantages : first, for perfect plane wave packets, the accuracy of the plane wave direction estimation can be analyzed in terms of $k \times r_0$ (see [2] and also section 2); second, it confers a rotational invariance property to the algorithm which is important to avoid amplitudes distortions depending on ray directions; and finally, dealing with periodic functions on a line (the circle) is cheaper than working with a surface field and allows the use of a fast algorithm (i.e. the `FFT`) to implement the filter.

However, as the field is not always available on the circle, gathering the observable may induce data preprocessing : interpolation procedure or one way extrapolation of the field if it is only known on a line, [1]. The preprocessing can add some noise to the data. This noise and/or linearization errors can pollute our data and possible instability of the original Dirichlet data `NMLA` method was a problem. A remedy, proposed in [2], used a L^2 Tychonov regularization, see also [13] for a L^1 regularization.

The first contribution of this paper is a more robust and simple resolution of the stability problem in the form of a different *impedance observable*. It modifies the filters and allows the mathematical derivation of a precise upper bound to the number of Fourier modes L_{kr_0} (defined in (4)) which guarantees stability. No other regularization is needed.

In the case of noisy plane wave data : we show in §2, using the stability property, that even for noise of the same order of amplitude as the signal, see conditions (9), the directions localization error is bounded by $\frac{\pi P}{L_{kr_0}+1}$, which asymptotically behaves as $O(\frac{1}{k})$, $k \sim \infty$. see (10) .

The `NMLA` method relies on the plane wave assumption (2). Therefore, arbitrary wave data is bound to carry linearization errors growing with the frequency. If second order terms estimate (the Hessian of the GO phase) were available, it would result in a better approximation of the high frequency GO rays directions and amplitudes.

In the case of perfect point source data in homogeneous space (Hankel functions), the phase is analytically known : this is the simplest "constant curvature" non linear wave data. Applying the `NMLA` filter we show in section §3.2 that the localization error induced

by the curvature (noted $\frac{1}{R}$) is controlled only if $L_{kr_0} < C\sqrt{k\,R}$ (C a pure constant). This constraint degrades the localization error accuracy to $O(\frac{1}{\sqrt{k\,R}})$, $k \sim \infty$.

Using Fast Multipoles Methods type techniques [9], we introduce in §3.3 a second order correction to the `NMLA` filters output. For an exact Hankel function the correction improves the localization error asymptotic behavior to $O(\frac{1}{(k\,R)^{\frac{3}{4}}})$, $k \sim \infty$. As we use this correction locally, it can be applied to general data. We simply assume that instead of the plane wave linearization we approximate the underlying high frequency solution by a constant curvature wavefront with an unknown virtual source. This correction to the classic `NMLA` filter leads to a second order accurate method, see the numerical results in [1] for applications in this direction.

§4 and 5 address more technical but practical issues.
§4 discusses the choice for the number of samples for the observable and also for the output of the `NMLA` filter. Remember that the output must be searched for maxima. In both case we show that these number must be larger than $2\,L_{kr_0} + 1$ and give precise usable formulae.
§5 introduces an additional Gaussian filtering procedure which aims at removing interferences between waves when there are more than one. This is important in view of angular decomposition of the observable as the "constant curvature" correction of §3 only works when the wave data radiates from a single source. Finally, a numerical illustration of these results is presented in §6.

2. Stable extraction of angles from noisy plane wave packets

2.1. A new impedance observable for `NMLA`

As discussed in the introduction, our new `NMLA` observable uses the impedance quantity on the measurement circle of radius r_0 centered at x_0,

$$U_k(\theta) = \left(\frac{1}{ik}\partial_{r_0} u_k(x) + u_k(x)\right), \quad x = x_0 + r_0\hat{s}, \quad \hat{s} = (\cos\theta, \sin\theta). \tag{3}$$

It is known that the knowledge of $U_k(\theta)$ and that u_k satisfies the Helmholtz equation inside the circle, is enough to reconstruct the whole solution since there is no resonance for an impedance Helmholtz problem : our observable contains hence all the information. As mentioned in the introduction, the observable in [2] was the restriction of u_k on the circle (compare (3) with (1)); this does not allow the reconstruction of the solution inside the circle for some exceptional values of k (resonance of the Dirichlet problem) and this deficiency underlies technical and practically important difficulties (stability in particular) which are removed by (3).

The `NMLA` filters B_k for the new observable are

$$\left\{\begin{array}{c} B_k U(\theta) = \dfrac{1}{2L_{kr_0}+1} \displaystyle\sum_{\ell=-L_{kr_0}}^{L_{kr_0}} \frac{(\mathcal{F}U)_\ell\; e^{i\ell\theta}}{(-i)^\ell (J_\ell(kr_0) - iJ'_\ell(kr_0))} \\ \text{with } L_{kr_0} = \max(1, [kr_0], \left[kr_0 + (kr_0)^{\frac{1}{3}} - 2.5\right]), \end{array}\right. \tag{4}$$

where $J_\ell(x)$ is the Bessel functions of order ℓ and argument x, $J'_\ell(x)$ their derivative and $(\mathcal{F}U)_\ell$ is the ℓ-th Fourier coefficient of U

$$(\mathcal{F}U)_\ell = \frac{1}{2\pi}\int_0^{2\pi} U(\theta)e^{-i\ell\theta}\,d\theta.$$

Note that the denominator in (4) never vanishes since $J_\ell(x)$ and $J'_\ell(x)$ have no common zeros, see [15, pp 479] or Equation (A.3) in the Appendix.

The filter formula comes as a generalization to arbitrary data of the inversion (7) of the expansion of the observable for plane waves (6). The formula for the number of terms in the sum L_{kr_0} is a necessary condition to the stability result stated in §2.2 and detailed in Appendix A .

2.2. Preliminary results for perturbed plane waves packets

We now assume noise perturbation of the plane wave data (2),

$$U_k(\hat{s}) = U_k^{plane}(\hat{s}) + \delta U(\hat{s}). \tag{5}$$

The first term corresponds to the plane wave packets, the second one to a random or correlated perturbation of u_k. The filters being linear we get

$$B_kU_k(\theta) = B_kU_k^{plane}(\theta) + B_k\delta U(\theta),$$

and as already noticed in [2] the part of U_k corresponding to the plane waves can be computed analytically; we have

$$B_kU_k^{plane}(\theta) = \sum_{p=1}^{P} b_p\Psi_{L_{kr_0}}(\theta-\theta_p),$$

where

$$\Psi_L(\varphi) = \frac{\sin((L+\frac{1}{2})\varphi)}{(2L+1)\sin\frac{\varphi}{2}}.$$

The proof relies on *the Jacobi Anger Expansion*, [10, page 66]; we have

$$\left(\frac{1}{ik}\partial_{r_0}+1\right)\left(e^{-ikr_0\cos(\theta-\theta_p)}\right) = \sum_{\ell=-\infty}^{\infty}\left(\frac{1}{ik}\partial_{r_0}+1\right)\left((-i)^\ell J_\ell(kr_0)e^{i\ell(\theta-\theta_p)}\right),$$

or

$$\left(\frac{1}{ik}\partial_{r_0}+1\right)\left(e^{-ikr_0\cos(\theta-\theta_p)}\right) = \sum_{-\infty}^{\infty}(-i)^\ell\left(-iJ'_\ell(kr_0)+J_\ell(kr_0)\right)e^{i\ell(\theta-\theta_p)}, \tag{6}$$

and, therefore,

$$B_k\left(\left(\frac{1}{ik}\partial_{r_0}+1\right)\left(e^{-ikr_0\cos(\theta-\theta_p)}\right)\right) = \frac{1}{2L_{kr_0}+1}\sum_{\ell=-L_{kr_0}}^{L_{kr_0}} e^{i\ell(\theta-\theta_p)} = \Psi_{L_{kr_0}}(\theta-\theta_p). \tag{7}$$

To understand how applying B_k to the observable provides a filtered output with peaks localized at the angles of incidence, we will use both the properties of the function $\Psi_L(\varphi)$ and a technical result that shows that one controls the norm of the operator B_k independently of the wavenumber k. We start with the properties of the function Ψ_L:

(i) $\Psi_L(\varphi)$ is even; its maximum is reached at $\varphi = 0$

$$\sup_{\varphi} \Psi_L(\varphi) = 1 = \Psi_L(0).$$

(ii) $\Psi_L(\varphi)$ take values in the range of its maximum only in the vicinity of 0; we have

$$|\Psi_L(\varphi)| > 0.45 \quad \Rightarrow \quad |\varphi| < \frac{2}{\sqrt{L(L+1)}}.$$

(iii) $\Psi_L(\varphi)$ is "small" far away from 0; we have

$$\Psi_L(\varphi) \leq \frac{\pi}{2L+1} \frac{1}{|\varphi|}.$$

Concerning the bound on the norm of the B_k operators, we have the following result :

Lemma 2.1 *There exists a pure constant $B^\star$ (i.e. independent of k) such that*

$$\sup_{\theta} |B_k U(\theta)| \leq \frac{B^\star}{\sqrt{2\pi}} \|U\|_{L^2(0,2\pi)} \leq B^\star \|U\|_{L^\infty(0,2\pi)}.$$

This result strongly depends on the choice of the Fourier mode truncation level L_{kr_0} in (4). Numerical experiments also show that we have

$$B^\star \leq 1, \text{ and, even a sharper } B^\star \leq 0.89,$$

if we deal with high frequencies such that $kr_0 > 3$.

These bounds on $B^\star$ mean that the filter operator does not amplify the noise too much.

The proof starts with Cauchy-Schwartz

$$|B_k U(\theta)| \leq \frac{1}{2L_{kr_0}+1} \left(\sum_{\ell=-L_{kr_0}}^{L_{kr_0}} \frac{1}{J_\ell^2(kr_0) + J_\ell'^2(kr_0)} \right)^{\frac{1}{2}} \left(\sum_{\ell=-\infty}^{\infty} |(\mathcal{F}U)_\ell|^2 \right)^{\frac{1}{2}},$$

then Parseval's equality to obtain

$$|B_k U(\theta)| \leq \left[\frac{1}{2L_{kr_0}+1} \left(\sum_{\ell=-L_{kr_0}}^{L_{kr_0}} \frac{1}{J_\ell^2(kr_0) + J_\ell'^2(kr_0)} \right)^{\frac{1}{2}} \right] \left(\frac{1}{2\pi} \int_0^{2\pi} |U(\varphi)|^2 \, d\varphi \right)^{\frac{1}{2}}, \quad (8)$$

and finally on a technical result (cf. appendix A) that shows that the term between square brackets is bounded independently of k under the condition on $L_{kr_0} = \max(1, [kr_0], \left[kr_0 + (kr_0)^{\frac{1}{3}} - 2.5\right])$ given in the definition of the filter (4).

2.3. Confidence interval for plane wave direction angle identification

We first address the single plane wave case $P = 1$. Let $\theta^\star$ denote the angle for which $\theta \mapsto B_k \left(b_1 e^{ikr_0 \cos(\theta_1 - \varphi)} + \delta U(\varphi) \right)(\theta)$ is maximum; we expect this will be the ray direction of the most energetic plane wave component. With the help of the stability property (Lemma 2.1), the accuracy of $\theta^\star$can be quantified :

Assuming that the noise level satisfies

$$\|\delta U\|_{L^\infty} < \frac{1}{4B^\star} |b_1|, \quad (9)$$

then the error on the angle estimation is given by

$$|\theta_1 - \theta^\star| \leq \frac{\pi}{L_{kr_0} + \frac{1}{2}} \sim O(\frac{1}{k}),\ k \sim \infty. \tag{10}$$

The proof is as follows :

$$B_k U_k(\theta) = b_1 \Psi_{L_{kr_0}}(\theta - \theta_1) + B_k \delta U.$$

Assuming $|\theta - \theta_1| > \frac{2\pi}{2L_{kr_0}+1}$, we use the third property of function $\Psi_{L_{kr_0}}$ and obtain

$$|B_k U_k(\theta)| \leq |b_1| \frac{\pi}{2L_{kr_0}+1} \frac{2L_{kr_0}+1}{2\pi} + B^\star \|\delta U\|_{L^\infty} \leq \frac{1}{2}|b_1| + B^\star \|\delta U\|_{L^\infty},$$

whereas, at $\theta = \theta_1$,

$$|B_k U_k(\theta_1)| \geq |b_1| - B^\star \|\delta U\|_{L^\infty}.$$

Thus, if the noise perturbation satisfies

$$2B^\star \|\delta U\|_{L^\infty} < \frac{1}{2}|b_1|, \tag{11}$$

the maximum of $|B_k U_{plane}(\theta)|$ will be reached in a confidence interval centered around θ_1 with size $\frac{\pi}{L_{kr_0}+\frac{1}{2}}$. When the frequency increases, since $L_{kr_0} \sim kr_0$, the width of this interval will diminish and the angle of incidence is recovered with more precision. We remark that inequality (11) is not very restrictive since a numerical estimate gives $\frac{1}{4B^\star} \simeq 0.28$: if the noise level does not surpass 28 % the angle will be detected within an interval of size $\sim \frac{2\pi}{kr_0}$.

Similar results can be derived for $P > 1$. The filter output combines sums of functions Ψ and the noise. The condition on the noise to guarantee a confidence interval will not only depend on the plane wave amplitudes, but also on their differences and on the separation interval between direction angles. For instance, if two plane waves have close direction angle and/or one of them has small amplitude small relative to the other, the noise and the interferences between the filtered outputs make its direction impossible to detect as a local maximum. We skip the precise mathematical results as they are technical, long and not essential.

Remark : L^∞ control of the noise.

Throughout the paper, the effect of the noise δU_k will be assumed to be controlled in the L^∞ norm.

The noise in the observable δU_k contains the *derivative* of the noise in $u_k(x)$ which could potentially be very large. However, for a wave like $u_k(x) \sim A(x)e^{ik\Phi(x)}$ with high k, we have $|\frac{1}{ik}\vec{\nabla}_x u_k(x)| \sim |\vec{\nabla}_x \phi(x) u_k(x)| = |u_k(x)|$ and the two terms in the definition of the observable are of the same order.

Therefore, when the observable is directly recorded, we can expect the noise in $\frac{1}{ik}\vec{\nabla}_x u_k(x)$ to be of same order than the noise in u_k. When $u_k(x)$ is computed on a grid of size h with some second order finite difference method, the numerical noise induced by the numerical approximation on $u_k(x)$ is in $O(kh)^2$ and the term $\frac{1}{ik}\vec{\nabla}_x u_k(x)$ can be obtained by centered finite differences with an error in $O(kh)$.

In both cases, it is sufficient to control δU_k in the L^∞ norm.

3. Source points identification using NMLA

3.1. Points sources viewed as local plane waves

After noisy plane wave packets (2), the simplest Helmholtz data are point sources solutions in homogeneous media. It is also a case we can handle analytically. Let us assume that the data is generated from a collection of P source points x_p with some additional random or correlated noise δu :

$$u_k(x) = \sum_{p=1}^{P} a'_p \frac{i}{4} H_0^{(1)}(k|x - x_p|) + \delta u(x), \qquad a'_p = a_p \sqrt{k}. \tag{12}$$

The additional $\sqrt{k}$ factor has been added to normalize the decay of $H_0^{(1)}(k|x-x_p|)$ when $k \to \infty$, $|x - x_p| \neq 0$. We have now $3 \times P$ unknowns : the a_p's, θ_p's and R_p's, where

$$x_p = x_0 + R_p \hat{s}_p. = x_0 + R_p(\cos\theta_p, \sin\theta_p).$$

When the frequency goes to infinity, we can substitute for the Hankel function its asymptotic development, [10, page 65]

$$u_k(x) = \sum_{p=1}^{P} a_p \frac{e^{ik|x_p - x|}}{\sqrt{-i\,8\pi|x_p - x|}} + \widetilde{\delta u}(x),$$

where the $\widetilde{.}$ indicates that the perturbation nows includes new asymptotic errors. If we want to use NMLA, a natural idea is to linearize the data on the observation circle $x_0 + r_0\hat{s}$ around the observation point x_0 to find our usual plane wave packet. If r_0 is "small enough" with respect to all the R_p's, we will have

$$u_k(x_0 + r_0\hat{s}) = \sum_{p=1}^{P} b_p\, e^{-ikr_0\cos(\theta - \theta_p)} + \widetilde{\widetilde{\delta u}}(x), \;\text{ with } b_p = a_p \frac{e^{ikR_p}}{\sqrt{-i\,8\pi R_p}}. \tag{13}$$

This means that, on the disk of center x_0 and radius r_0, the high frequency field is the sum of P plane waves plus some noise perturbation. The next step is to apply the previous filter (i.e. our operator B_k) to the impedance quantity (3). However, we need to be careful about the errors accumulated over the successive approximations (see the number of tildes rising over the perturbation term !).

If we only focus on the linearization error, we see that we used one term for the modulus and two terms for the phase in the expansion

$$\begin{aligned} k|x_p - x| \;&=\; k|x_p - x_0| - k(x - x_0)\cdot\hat{s}_p \\ &\quad + \frac{k}{2|x_p - x_0|}\left(|x - x_0|^2 - (x - x_0\cdot\hat{s}_p)^2\right) + \ldots, \end{aligned}$$

or, for $x = x_0 + r_0\hat{s}$

$$k|x_p - (x_0 + r_0\hat{s})| = kR_p - kr_0\cos(\theta - \theta_p) + \frac{kr_0^2}{2R_p}\sin^2(\theta - \theta_p) + \ldots \tag{14}$$

For a fixed radius r_0, since the second order term goes to infinity with k, the NMLA filter is likely to fail. One would like to scale down the radius r_0 with the frequency to control it. However, we saw in §2.3 that the accuracy of the angle extraction decreases with the truncation level L_{kr_0} which is $O(k\,r_0)$ for large k. In the next section, we perform a mathematical analysis of this phenomena.

3.2. Analysis of a `NMLA` *filtered source point*

We simplify and assume that the data field corresponds to a unique source point x_1 :

$$u_k(x) = a_1 \sqrt{k}\, \frac{i}{4} H_0^{(1)}(k|x - x_1|) + \delta u(x).$$

Then, we use the *Graff addition Theorem*, [10, page 66]: when r_0 is smaller than $R_1 = |x_1 - x_0|$, we have

$$u_k(x_0 + r_0\hat{s}) = a_1 \sqrt{k}\, \frac{i}{4} \sum_{\ell=-\infty}^{+\infty} H_\ell^{(1)}(kR_1) J_\ell(kr_0)\, e^{i\ell(\theta-\theta_1)} + \delta u(x_0 + r_0\hat{s}),$$

where θ (resp. θ_1) is the angle associated to $\hat{s}$ (resp. to $\frac{x_1-x_0}{|x_1-x_0|}$). The impedance quantity on the circle with the usual noise perturbation is

$$U_k(\theta) = U_k^{pt}(\theta) + \delta U(\theta),$$

where

$$\begin{aligned} U_k^{pt}(\theta) &= (\frac{1}{ik}\partial_{r_0} + 1) u_k(x_0 + r_0\hat{s}) \\ &= a_1\sqrt{k}\, \frac{i}{4} \sum_{\ell=-\infty}^{+\infty} H_\ell^{(1)}(kR_1)(J_\ell(kr_0) - iJ'_\ell(kr_0))\, e^{i\ell(\theta-\theta_1)}, \end{aligned}$$

or, after a change of variable

$$U_k^{pt}(\theta) = a_1 \frac{e^{ikR_1}}{\sqrt{-i\, 8\pi R_1}} \sum_{\ell=-\infty}^{+\infty} C_\ell(kR_1)\, (-i)^\ell (J_\ell(kr_0) - iJ'_\ell(kr_0))\, e^{i\ell(\theta-\theta_1)},$$

with

$$C_\ell(kR_1) = i^\ell \sqrt{\frac{ik\pi R_1}{2}}\, e^{-ikR_1}\, H_\ell^{(1)}(kR_1). \tag{15}$$

It is important to notice that when kR_1 is large enough $C_\ell(kR_1)$ is a perturbation of 1 due to the asymptotic expansion [15, page 198],

$$C_\ell(kR_1) \sim 1 + \sum_{m=1}^{\infty} \frac{(\ell, m)}{(-2ikR_1)^m}, \tag{16}$$

$$\text{with } (\ell, m) = \frac{(4\ell^2 - 1^2)(4\ell^2 - 3^2)\dots(4\ell^2 - (2m-1)^2)}{2^{2m} m!}.$$

The zeroth order approximation $C_\ell(kR_1) \sim 1$ corresponds to a plane wave linearization of the data. As in §2.2, the `NMLA` filter will map it to the shape function $\Psi_{L_{kr_0}}(\theta - \theta_1)$. If we split the data between linear and remaining quantities we obtain (cf. Definition of b_1 in (13) and the expression of the filter B_k in (4))

$$\begin{aligned} B_k U_k^{pt}(\theta) &= b_1 \tfrac{1}{2L_{kr_0}+1} \textstyle\sum_{-L_{kr_0}}^{L_{kr_0}} C_\ell(kR_1)\, e^{i\ell(\theta-\theta_1)} \\ &= b_1 \Psi_{L_{kr_0}}(\theta - \theta_1) + \delta\beta(\theta), \text{ where} \end{aligned} \tag{17}$$

$$\delta\beta(\theta) = b_1 \frac{1}{2L_{kr_0}+1} \sum_{-L_{kr_0}}^{L_{kr_0}} (C_\ell(kR_1) - 1)\, e^{i\ell(\theta-\theta_1)}. \tag{18}$$

$\delta\beta$ is precisely the image of the linearization error by the filter. It can be bound as follows

$$|\delta\beta(\theta)| \leq |b_1| \left(\frac{1}{2L_{kr_0}+1} \sum_{\ell=-L_{kr_0}}^{L_{kr_0}} |C_\ell(kR_1) - 1| \right) = |b_1|\, \mathcal{E}(L_{kr_0}, kR_1).$$

For noisy source point data, we get

$$B_k U_k(\theta) = b_1 \Psi_{L_{kr_0}}(\theta - \theta_1) + \delta\beta(\theta) + B_k \delta U(\theta).$$

We then apply the result of §2.3 where we filter to the impedance data linked to a unique noisy source point. The only difference is the additional linearization noise which modifies condition (11). The supremum of this function will correspond to an angle located at a distance less than $\frac{\pi}{L_{kr_0}+\frac{1}{2}}$ of θ_1, as soon as

$$2B^\star \|\delta U\|_{L^\infty} + 2|b_1|\mathcal{E}(L_{kr_0}, kR_1) \leq \frac{|b_1|}{2}. \tag{19}$$

So, L_{kr_0} controls the direction localization error but we also need $\mathcal{E}(L_{kr_0}, kR_1)$ to be small. It induces a new constraint on L_{kr_0} depending on $k\,R_1$. We found numerically that, for $\mathcal{E}(L_{kr_0}, kR_1)$ to remain bounded by, lets say $\epsilon = 10^{-1}$, 10^{-2} or 10^{-3}, and independently of k, L_{kr_0} must approximately satisfy the respective inequalities (with some approximations)

$$L_{kr_0} \leq C_\epsilon \sqrt{kR_1} \quad \text{with } C_{0.1} = 0.775,\ C_{0.01} = 0.25 \quad C_{0.001} = 0.0775. \tag{20}$$

The $\sqrt{kR_1}$ dependency is not surprising when we look at the second order term neglected in the Taylor development of the phase (14).

Note that inequality (20) is not unconditionally satisfied when r_0 is fixed and k is too large. To fix this problem one may try to choose a k dependent r_0 satisfying

$$kr_0 + (kr_0)^{\frac{1}{3}} - 2.5 \leq C_\epsilon (kR_1)^{\frac{1}{2}}.$$

Asymptotically r_0 must go to zero like $r_0 \sim \frac{1}{4}\sqrt{\frac{R_1}{k}}$ note the observation circle radius shrinks with k. When R_1 is unknown (we recall that we only need local data near the observation point) this formula is not practical, but we can replace R_1 by R_-, any estimate from below of this distance. Most important, choosing a radius r_0 which decreases like the square root of the wavenumber will induce a decrease of L_{kr_0} and, consequently, of the accuracy in localization of the peak, i.e. of the angle of incidence.

In **summary :** for all $\epsilon > 0$, and all $R_- > 0$ there exists C_ϵ such that when

$$L_{kr_0} \leq C_\epsilon \sqrt{kR_-} \tag{21}$$

holds then

$$\mathcal{E}(L_{kr_0}, kR_1) \leq \epsilon, \quad \forall R_1 \geq R_-. \tag{22}$$

in particular, using (19), and assuming that ϵ and the noise level are small enough in the sense that

$$\|\delta U\|_{L^\infty} \leq \frac{|b_1|(1-4\epsilon)}{4B^\star}, \quad b_1 = a_1 \frac{e^{ikR_1}}{\sqrt{-i\,8\pi R_1}},$$

the angle $\theta^\star$ for which

$$\theta \mapsto B_k \left(a_1 \sqrt{k}\, \frac{i}{4} H_0^{(1)}(k\sqrt{R_1^2 + r_0^2 - 2R_1 r_0 \cos(\varphi - \theta_1)}) + \delta U(\varphi) \right)(\theta)$$

is maximum satisfies $|\theta_1 - \theta^\star| < \frac{\pi}{L_{kr_0}+\frac{1}{2}}$.

For large k, when the radius of the observation circle is chosen like $r_0 \sim C_\epsilon\sqrt{\frac{R_-}{k}}$, $|\theta_1 - \theta^\star|$ decreases like $\frac{\pi}{C_\epsilon\sqrt{kR_-}}$.

In the next §3.3, we show that on can use more terms in the asymptotic series (16) to correct the `NMLA` filter up to second order.

3.3. Second order correction of the filter for a source point

We saw in the previous sections that the good angle localization property obtained for noisy plane wave data does not carry over to point source data. We also know that the linearization is responsible for this loss of accuracy. Roughly speaking, the localization is in $\frac{C}{k}$ for a plane wave and $\frac{C'}{\sqrt{k}}$ for the source point. This section shows that it is possible to identify the curvature from the filtered image of the observable and then use it to improve the angle extraction.

We drop the noise for now and apply `NMLA` to the impedance data associated to a source point. We then get (using the maximum test) a first estimate of the true angle $\theta_1 = \frac{x_1-x_0}{|x_1-x_0|}$; this first estimation is denoted θ_{est}. Meanwhile, we have an analytical formula for the Fourier coefficients $\hat{\beta}_\ell$ of $B_k U_k^{pt}(\theta)$ given by (see (17))

$$\hat{\beta}_\ell = \frac{b_1}{2L_{kr_0}+1} C_\ell(kR_1)\, e^{-i\ell\theta_1}.$$

We shift the phase for convenience,

$$\hat{\beta}_\ell e^{i\ell\theta_{est}} = \frac{b_1}{2L_{kr_0}+1} C_\ell(kR_1)\, e^{i\ell(\theta_{est}-\theta_1)} = \frac{b_1}{2L_{kr_0}+1} C_\ell(kR_1)\, e^{i\ell\delta\theta},$$

where $\delta\theta = \theta_{est} - \theta_1$ is the error we make on the angle. We now use the first two terms in the asymptotic series (16)

$$C_\ell(kR_1) \simeq \frac{e^{i\frac{\ell^2-\frac{1}{4}}{2kR_1}}}{\left(1-\frac{\ell^2-\frac{1}{4}}{(kR_1)^2}\right)^{\frac{1}{4}}}, \tag{23}$$

and obtain

$$\hat{\beta}_\ell e^{i\ell\theta_{est}} = \frac{b_1}{2L_{kr_0}+1} e^{i\left(\ell\delta\theta+\frac{\ell^2-\frac{1}{4}}{2kR_1}\right)} \frac{1}{\left(1-\frac{\ell^2-\frac{1}{4}}{(kR_1)^2}\right)^{\frac{1}{4}}} + O(\frac{1}{(kR_1)^3}).$$

If we consider($\Im$ stands for imaginary part)

$$\varphi_\ell = \Im\left(\log(\hat{\beta}_\ell e^{i\ell\theta_{est}}) - \log(\hat{\beta}_0)\right) \simeq \ell\delta\theta + \frac{\ell^2}{2kR_1}, \tag{24}$$

we see that we get a parabolic deviation of the phase (see Figure 2 for an example). A simple correction process therefore consists in computing the closest parabola (for instance in the least square sense) of $\ell \mapsto \varphi_\ell$ for $|\ell| \leq L_{kr_0}$. A weighted optimization can be used to take into account that the asymptotic is more accurate for small ℓ's. The estimated parabola coefficients $\delta\theta_{est}$ and R_{est} provide a correction on the angle and an estimation of the distance to the source or, equivalently, of the front curvature.

These, in turn can be used to construct a corrected filter,

$$B_k^{cor}U(\theta) = \frac{1}{2L_{kr_0}+1}\sum_{\ell=-L_{kr_0}}^{L_{kr_0}} \frac{(\mathcal{F}U)_\ell\; e^{i\ell\theta}\hat{C}_\ell^{cor}}{(-i)^\ell(J_\ell(kr_0)-iJ'_\ell(kr_0))} \tag{25}$$

$$\text{with } \hat{C}_\ell^{cor} = e^{-i\ell\left(\delta\theta_{est}+\frac{\ell^2-\frac{1}{4}}{2kR_{est}}\right)}\left(1-\frac{\ell^2-\frac{1}{4}}{(kR_{est})^2}\right)^{\frac{1}{4}},$$

which gives better localization as the parabolic deviation of the phase of $\hat{\beta}_\ell$ has been removed. Remark that $\left|\hat{C}_\ell^{cor}\right| \leq 1$, and so the uniform stability estimate in k of the norm of B_k (11) also holds for B_k^{cor}, $\|B_k^{cor}\| \leq B^\star$ independent of k again as long as $L_{kr_0} = \max(1, [kr_0], [kr_0 + (kr_0)^{\frac{1}{3}} - 2.5])$.

The modified corrected filter will yield a better result only if the error induced by approximation (23) is small enough to not perturb the value of the maximum too much. Using the approach described in the previous section, we have to make sure that

$$\mathcal{E}'(kR_1, L_{kr_0}) = \left(\frac{1}{2L_{kr_0}+1}\sum_{\ell=-L_{kr_0}}^{L_{kr_0}}\left|C_\ell(kR_1) - \frac{e^{i\frac{\ell^2-\frac{1}{4}}{2kR_1}}}{\left(1-\frac{\ell^2-\frac{1}{4}}{(kR_1)^2}\right)^{\frac{1}{4}}}\right|\right) \leq \epsilon, \tag{26}$$

where we used the truncation, now up to second order, of the asymptotic series (16). Again, we performed numerical computations which show that when $kR_1 > 4.25$ then (26) is satisfied when $L_{kr_0} + 1 \leq C'_\epsilon(kR_1)^{\frac{3}{4}}$, with $C'_\epsilon = 1.75,\ 1.05,\ 0.59$, for ϵ equals to 10^{-1}, 10^{-2}, 10^{-3}. Corrected `NMLA` will only succeed if

$$kr_0 + (kr_0)^{\frac{1}{3}} \leq C'_\epsilon(kR_1)^{\frac{3}{4}}.$$

The radius must asymptotically behaves like $r_0 \sim C'_\epsilon \frac{R_1^{\frac{3}{4}}}{k^{\frac{1}{4}}}$. The confidence interval $\frac{\pi}{L_{kr_0}+\frac{1}{2}}$ for angle localization (see §3.2) is improved and varies now like $\frac{\pi}{C'_\epsilon(kR_-)^{\frac{3}{4}}}$.

Remark on filtering non circular waves :

All this procedure can be applied when the wavefield does not correspond to a point source. The key point is to realize that up to higher order terms, any asymptotic curved 2-D wavefield u_k is equivalent to a point source; if $u_k(x) \simeq A(x)e^{ik\phi(x)}$ in a neighborhood of a point x_0, we have

$$u_k(x) \simeq \left[A(x_0)e^{ik\phi(x_0)}\sqrt{-i8\pi R(x_0)}e^{-ikR(x_0)}\right]\sqrt{k}\,\frac{i}{4}H_0^{(1)}\left(k\,|x - x_s(x_0)|\right),$$

where $R(x_0)$ is the curvature of the wavefront at point x_0 and $x_s(x_0)$ is the fictitious point source $x_s = x_0 + R(x_0)(\cos\theta_0, \sin\theta_0)$, θ_0 the direction of $\vec{\nabla}\varphi(x_0)$.

4. Discretization parameters

In practice, in the `NMLA` filter (4), the Fourier transform is replaced by a discrete Fourier transform which we compute with a Fast Fourier Transform algorithm. Let N be the

number of observed samples on the circle, then the operator B_k^N, a discrete approximation of the filter B_k, is given by

$$\left\{ \begin{array}{l} B_k^N U(\theta) = \dfrac{1}{2L_{kr_0}+1} \displaystyle\sum_{\ell=-L_{kr_0}}^{L_{kr_0}} \dfrac{(\mathcal{F}_N U)_\ell \; e^{i\ell\theta}}{(-i)^\ell (J_\ell(kr_0) - iJ'_\ell(kr_0))} \\ \qquad \text{with } L_{kr_0} = \max(1, [kr_0]\,, \Big[kr_0 + (kr_0)^{\frac{1}{3}} - 2.5\Big]), \end{array} \right. \tag{27}$$

with

$$(\mathcal{F}_N U)_\ell = \frac{1}{N} \sum_{p=1}^{N} U(\theta_p) e^{-i\ell\theta_p}, \qquad \text{with } \theta_p = \frac{2\pi(p-1)}{N}.$$

Clearly, we need $N \geq 2L_{kr_0}+1$. We show in §4.1 that the stability result of §2 still holds and give a lower bound for N to preserves the angle localization error obtained for the continuous filter (4). Even though this bound behaves as $2L_{kr_0}+1$ asymptotically in k, in practice it leads to a larger number.

We also need to determine a number of sample Q for the output of the filter $B_k^N U$. Again we must have $Q > 2L_{kr_0}+1$ and Q large enough to capture with sufficient precision the angle corresponding to the maximum or maxima of the modulus of the filtered image. In section §4.2 we give a practical formula for Q depending on N which preserves the localization error.

4.1. Discretization of the observable

Let N be an integer larger than $2L_{kr_0}+1$; we consider the discrete approximation of the filter B_k^N defined by (27) above. A straightforward calculation shows that the estimate of the norm of B_k remains true for B_k^N; indeed, we have, by following the inequality of the continuous case,

$$\left|B_k^N U(\theta)\right| \leq \frac{1}{2L_{kr_0}+1} \left(\sum_{\ell=-L_{kr_0}}^{L_{kr_0}} \frac{1}{J_\ell^2(kr_0) + J_\ell'^2(kr_0)} \right)^{\frac{1}{2}} \left(\sum_{\ell=-L_{kr_0}}^{L_{kr_0}} \left|\left(\mathcal{F}^N U\right)_\ell\right|^2 \right)^{\frac{1}{2}},$$

then, since $2L_{kr_0}+1$ is assumed less than N, the discrete Parseval equality provides

$$\left|B_k^N U(\theta)\right| \leq \frac{1}{2L_{kr_0}+1} \left(\sum_{\ell=-L_{kr_0}}^{L_{kr_0}} \frac{1}{J_\ell^2(kr_0) + J_\ell'^2(kr_0)} \right)^{\frac{1}{2}} \left(\frac{1}{N} \sum_{p=1}^{N} |U(\theta_p)|^2 \right)^{\frac{1}{2}},$$

or, bounding the term between square brackets by $B_\star$ (cf. appendix) and each sample $|U(\theta_p)|$ by the maximum of $|U|$

$$\left|B_k^N U(\theta)\right| \leq B^\star \|U\|_{L^\infty(0,2\pi)}.$$

To evaluate the number of samples necessary to a good approximation, we split the observable as follows

$$U(\theta) = U_N(\theta) + U_N^\perp(\theta), \quad U_N(\theta) = \sum_{\ell=-M}^{M} (\mathcal{F}U)_\ell \, e^{i\ell\theta}, \text{ with } M = \frac{N-1}{2}.$$

We remark that (since $M > L_{kr_0}$) the Fourier coefficients of U_N are calculated exactly by our equidistributed quadrature rule; we have $(\mathcal{F}_N U_N)_\ell = (\mathcal{F}U_N)_\ell$, which implies that $B_k^N U_N$ coincides with $B_k U_N$. Thus,

$$\begin{aligned} B_k^N U(\theta) &= B_k^N U_N(\theta) + B_k^N U_N^\perp(\theta) = B_k U_N(\theta) + B_k^N U_N^\perp(\theta) \\ &= B_k U(\theta) + (B_k^N - B_k) U_N^\perp(\theta); \end{aligned}$$

but since $B_k U_N^\perp$ vanishes (as $M > L_{kr_0}$ again), it remains

$$B_k^N U(\theta) = B_k U(\theta) + B_k^N U_N^\perp(\theta),$$

whence

$$|B_k^N U(\theta) - B_k U(\theta)| \leq B^\star \sup_\theta |U_N^\perp(\theta)|.$$

Assuming that N is large enough for the sup of the remaining part to be small, we have that the function $B_k^N U(\theta)$ is, when $U(\theta)$ is the trace of some perturbed plane waves, the weighted sum of a linear combination of sinc like functions $\Psi_{L_{kr_0}}(\theta - \theta_p)$ plus a perturbation (sum of the noise raised with the error induced by the discretization).

It is then possible to proceed again as in §2.3; for instance, if U is the observable associated to a perturbed plane wave $b_1 e^{-ikr\cos(\theta-\theta_1)} + \delta U$, assuming that N is large enough to have, for ϵ small given,

$$\sup_\theta |U_N^\perp(\theta)| \leq \epsilon |b_1|, \tag{28}$$

then the supremum is reached at a point $\theta^\star$ localized in a confidence interval of size $\frac{\pi}{L_{kr_0}+\frac{1}{2}}$ around θ_1 when $|b_1| - B^\star\|\delta U\| - \epsilon|b_1|$ is greater than $\frac{|b_1|}{2} + B^\star\|\delta U\| + \epsilon|b_1|$, or

$$\|\delta U\|_\infty \leq |b_1| \frac{1-4\epsilon}{4B^\star}. \tag{29}$$

According to Equation (6), Condition (28) is equivalent to find N large enough to have

$$\sup_\theta \left| \sum_{\ell > M} (J_\ell(kr_0) - iJ_\ell'(kr_0))(-i)^\ell \cos \ell\theta \right| \leq \frac{\epsilon}{2}, \quad N = 2M+1. \tag{30}$$

This problem has been the subject of many studies in the framework of the "*Fast Multipole Method*". For instance, using the techniques developed in [6], it can be shown that when kr_0 is larger than 10 then, when $N > 2M^\epsilon(kr_0) + 1$ with

$$M^\epsilon(kr_0) = \left[kr_0 + \frac{1}{2} \left(\frac{3}{2} W\left(\frac{2}{3\pi\epsilon^2} \right) \right)^{\frac{2}{3}} (kr_0)^{\frac{1}{3}} \right] + 2\,, \tag{31}$$

then (30) holds. The function $W(u)$ is the *Lambert function* defined implicitly by

$$W(u) e^{W(u)} = u \tag{32}$$

(it has a sub-logarithmic behavior when u tends toward infinity). A numerical study shows that the constant depending on the Lambert function in front of $(kr_0)^{\frac{1}{3}}$ in (31) is, respectively, 3.24, 49.37 and 156.01 for $\epsilon = 10^{-2}$, $\epsilon = 10^{-6}$ and $\epsilon = 10^{-10}$. So it is always necessary to choose $N > 2L_{kr_0} + 1$, that is twice more samples than Fourier coefficients.

In practice: We take $N \sim 2M^\epsilon(kr_0) + 1$ with ϵ such that the upper bound in (29) is a small perturbation of (9). Note that choosing ϵ very small does not affect the asymptotic for k large since the asymptotic of N and $2L_{kr_0}$ are the same, i.e. $\sim 2kr_0$.

Remark: The same approach can be followed to study the discretization in the point source case, assuming that the distance to the point source is controlled ($R_1 \geq R_-$). Ones uses in this case truncation error estimates in the Graff series that have been also studied in the *Fast Multipole Method*. The estimates for the $M^\epsilon(kr_0)$ are of the same kind but with ϵ^2 replaced by $(1-\frac{r_0}{R_-})\epsilon^2$ in (31), see [5].

4.2. Taking the maximum over a finite set of samples

The natural and practical post processing of the `NMLA` output consists in selecting the supremum of B_kU_k over a finite number of discretization angles. We are interested here in the evaluation of the number of samples Q needed to capture it accurately.

First, we know that before discretization, the size of the confidence interval linked to the truncation to $2\,L_{kr_0}+1$ is $\frac{\pi}{L_{kr_0}+\frac{1}{2}}$. So a uniform discretization of size Q should be chosen such that there is least one sample in every interval of this length. We need

$$Q \geq 2L_{kr_0}+1.$$

Let us proceed for a single plane wave; the discretization of the image of the `NMLA` operator is

$$B_kU_k(\theta_q^Q) = b_1\Psi_{L_{kr_0}}(\theta_q^Q-\theta_1)+\delta U(\theta_q^Q), \quad \theta_q^Q = \frac{2\pi(q-1)}{Q}.$$

We use the properties of function $\Psi_{L_{kr_0}}$ as in §2.3. For θ_q^Q outside the interval $|\theta_q^Q-\theta_1| \leq \frac{\pi}{L_{kr_0}+\frac{1}{2}}$, we have

$$|B_kU_k(\theta_q^Q)| \leq \frac{1}{2}|b_1| + B^\star\|\delta U\|_{L^\infty}.$$

For θ_q^Q inside this interval, the supremum of our discretization is bounded below by the value taken at the sampled angle the closest to θ_1, denoted $\theta_{q_0}^Q$; therefore

$$|B_kU_k(\theta_{q_0}^Q)| \geq |b_1|\Psi_{L_{kr_0}}(\delta\theta) - B^\star\|\delta U\|_{L^\infty},$$

where $\delta\theta = \theta_{q_0}^Q-\theta_1$. We have necessarily $|\delta\theta| \leq \frac{\pi}{Q}$, and the inequality is an equality when the angle θ_1 is exactly at the middle of two samples.

Now, when Q is large enough, $\delta\theta$ is close to 0 and so $\Psi_{L_{kr_0}}(\delta\theta)$ is close to 1. Indeed, we have

$$\Psi_{L_{kr_0}}(\delta\theta) = \frac{\sin[(L_{kr_0}+\frac{1}{2})\delta\theta]}{(L_{kr_0}+\frac{1}{2})\delta\theta} \geq 1-\frac{1}{6}\left((L_{kr_0}+\frac{1}{2})\delta\theta\right)^2,$$

which is bounded by below by $1-\frac{1}{2}\left(\frac{\pi}{\sqrt{3}}\frac{Lk+\frac{1}{2}}{Q}\right)^2$ since $|\delta\theta| \leq \frac{\pi}{Q}$. Consequently, for ϵ given, when Q is such that

$$Q > Q_\epsilon := (L_{kr_0}+\frac{1}{2})\frac{\pi}{\sqrt{3\epsilon}}, \tag{33}$$

then, $\Psi_L(\delta\theta) \geq (1-\frac{\epsilon}{2})$ and

$$|B_kU_k(\theta_{q_0}^Q)| \geq (1-\frac{\epsilon}{2})|b_1| - B_\star\|\delta U\|_{L^\infty}.$$

We conclude: $|\theta^Q_{q0} - \theta_1|$ will be less than $\frac{\pi}{L_{kr_0}+\frac{1}{2}}$ when the second term of the inequality above is greater than $\frac{1}{2}|b_1| + B_\star\|\delta U\|_{L^\infty}$, i.e. when

$$\|\delta U\|_{L^\infty} \leq \frac{|b_1|(1-\epsilon)}{4B^\star} \tag{34}$$

Condition (34) is not changed too much compared to condition (9) of the continuous case when ϵ is small, says, $\epsilon = 10^{-1}$.

In Practice : From practical considerations, linked to the use of the `FFT`, we propose to take $Q = Q_a = 2^a N$, N the number of samples of the previous section and a chosen the smallest to have $2^a N > Q_{\epsilon=0.1}$, Q_ϵ given in (33). Asymptotically, for very large k, since $N \sim 2(L_{kr_0} + \frac{1}{2})$, we find $a = 2$, $Q = 4N$ and the number of samples for the image of the filter grows linearly like $8kr_0$.

5. An extension: the Gaussian weights filter

In the case of multiple plane waves or point sources arriving at the observation with angles θ_n, the `NMLA` output is a sum of functions $\Psi_L(\theta - \theta_n)$. These functions decrease like $\frac{\pi}{(2\,L+1)|\theta-\theta_n|}$, which may be not fast enough to avoid pollution of the (local) maxima identification for each branch of the data when angles are close.

Even though this will not change the decay rate in $\frac{1}{|\theta-\theta_n|}$, we try to improve the constant though a convolution with a smooth Gaussian window. It smooths the Ψ_L functions and preserves the maxima location.

The modification is easily incorporated into the filter by a multiplication in the Fourier space

$$\left\{ \begin{array}{c} B^g_k U(\theta) = \dfrac{1}{2L_{kr_0}+1} \displaystyle\sum_{\ell=-L_{kr_0}}^{L_{kr_0}} \dfrac{(\mathcal{F}U)_\ell\, \varpi^k_\ell\, e^{i\ell\theta}}{(-i)^\ell (J_\ell(kr_0) - iJ'_\ell(kr_0))} \\ \text{with } L_{kr_0} = \max(1, [kr_0], \Big[kr_0 + (kr_0)^{\frac{1}{3}} - 2.5\Big]), \end{array} \right. \tag{35}$$

with

$$\varpi^k_\ell = \frac{\hat{G}^k_\ell}{\nu_k}, \quad \nu_k = \frac{1}{2L_{kr_0}+1} \sum_{\ell=-L_{kr_0}}^{L_{kr_0}} \hat{G}^k_\ell, \tag{36}$$

where $\hat{G}^k_\ell$ are real positive and even coefficients. We decided to use the Fourier coefficients of a Gaussian function $G^k(\theta)$ (τ is a free parameter)

$$\hat{G}^k_\ell = e^{-\frac{1}{2}\left(\frac{\ell}{\tau L_{kr_0}}\right)^2}. \tag{37}$$

As

$$\left|\hat{G}^k_\ell\right| < 1, \quad \lim_{L_{kr_0}\to\infty} \nu_k = \tau \int_0^{\frac{1}{\tau}} e^{-\frac{1}{2}\xi^2} d\xi,$$

we infer that there exists some number C_τ, independent of k such that

$$\sup_k \max_{\ell,\ |\ell|\leq L_{kr_0}} \varpi^k_\ell \leq C_\tau,$$

and get the bound

$$\max_\theta |B_k^g U(\theta)| < B^\star C_\tau \max_\theta |U(\theta)| .$$

The new Gaussian weighted filter (35)-(36)-(37) enjoys the same stability properties as the original `NMLA` filter. We have good control over noise.

If we apply it to a plane wave packet we obtain

$$B_k^g U_k^{plane}(\theta) = \sum_{p=1}^{P} b_p \Psi^\tau_{L_{kr_0}}(\theta - \theta_p),$$

where the new shape function $\Psi_{L_{kr_0}}$ is the convolution of the original one with the Gaussian

$$\Psi_{L_{kr_0}} \star G^k(\theta) = \Psi^\tau_{L_{kr_0}}(\theta) = \left(\sum_{\ell=-L^k}^{L_{kr_0}} \hat{G}^k_\ell \right)^{-1} \sum_{\ell=-L_{kr_0}}^{L_{kr_0}} \hat{G}^k_\ell e^{i\ell(\theta-\theta_p)}.$$

Figure 1 illustrates numerically the effect of the Gaussian filter for $P = 2$. The decay seems slightly improved and we also notice that the amplitude of the maximum is more accurate.

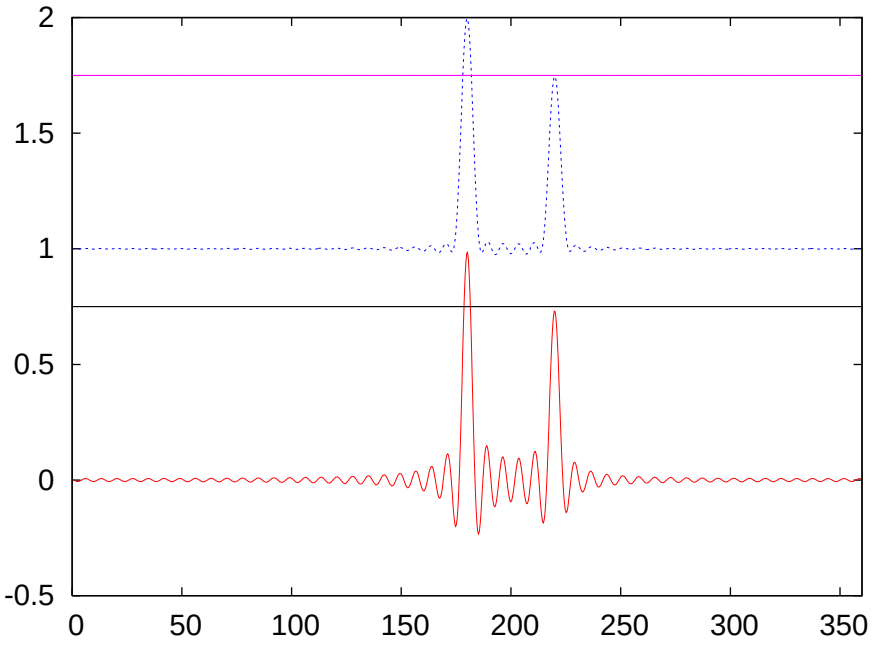

Figure 1. Comparison of $B_k(U_k)$ and $1 + B_k^g(U_k)$ when U_k is the observable associated to $u_k(x) = e^{ikr_0\cos(\theta-\pi)} + \frac{3}{4}e^{ikr_0\cos(\theta-\frac{11\pi}{9})}$. The amplitude $\frac{3}{4}$ is recovered with more precision with the Gaussian Filter.

6. Numerical study

The aim of this section is to demonstrate on very simple (and academic) examples the validity of our approach. More sophisticated and concrete examples can be found in [1].

6.1. Noisy synthetic point source data

We use the exact solution in homogeneous space, the Hankel function. The observation point x_0 is at a distance $R = 1$ meter from the source point in the direction $(\cos\theta_i, \sin\theta_i)$. We arbitrarily chose $\theta_i = 157.77$ degrees.

In order to add correlated noise, we proceed as follows : we introduce a regular Cartesian grid on top of the observation circle. The grid step is $h = \frac{2\pi}{k}\frac{1}{n_\lambda^g}$ where k is the wave number. We use $n_\lambda^g = 5$ and $n_\lambda^g = 10$ for strong and weak noise. The data values are not taken exactly at the points uniformly sampled on the observation circle but at their closest grid points inducing correlated noise.

6.2. The test algorithm for the curvature correction

Our algorithm requires a rough estimate by below of the distance R_1 between the source point and the observation point x_0: here, we assume that the source is located somewhere outside a circle centered at x_0 with radius $R_- = 0.5R_1 = 0.5$ meter. Second, for each wavenumber k we need to choose the radius of the observation circle $r_0 = r_0(k)$. To do that, we determine L_k the largest L such that

$$\mathcal{E}'(kR_-, L) \simeq 0.01,$$

$\mathcal{E}'$ given in (26). On the considered wavelength interval, we find

$$L_k \simeq 0.93(kR_-)^{0.763}.$$

Then we define the radius of the observation circle $r_0 = r_0(k)$ as the unique solution of

$$L_k = kr_0 + (kr_0)^{\frac{1}{3}} - 2.5.$$

Note that the filter integer truncation level L_{kr_0} is the integer part of the real number L_k.

The observation points are uniformly sampled on the circle $\mathcal{C}(x_0, r_0)$ and then projected onto the "noise" grid. We take $P = 2M^\epsilon(kr_0) + 2$ points where $M^\epsilon(kr_0)$ is given by (31) where $\epsilon = 10^{-13}$. Then we apply the `NMLA` discrete filter (4) on this data and select the angle corresponding to the maximum modulus

$$\beta_q = B_k^Q U_k\left(\frac{2\pi(q-1)}{Q}\right) \text{ for } p = 1, \ldots, Q$$

Following §4.2, we choose $Q = 4\,P$.

We then perform the curvature analysis of §3.3. We compute the phase φ_ℓ defined by (24) being careful to unwrap the possible 2π rotations (we assume the phase cannot jump more than $\frac{\pi}{2}$ between two successive ℓ).

There are different possible ways to perform the parabolic fit of $\ell \to \varphi_\ell$. First, we observe that the parabolic deviation is less accurate as $|\ell|$ grows, see asymptotic (16). Thus, if we consider only the Fourier coefficients ℓ such that $|\ell|$ is bounded by some $L < L_{kr_0}$, this would lead us to take L small. However, the noise affects the parabolic shape and the only way to control that noise effect is to take L large. Finally, we do as follows : for two successive values of L_e, $L_e = \frac{L_{kr_0}}{2}$, $\frac{L_{kr_0}}{2} + 1$, we find the best least square parabolic fit of φ_ℓ between $-L_e$ and L_e. It determines three polynomial coefficients : the

zeroth order term is a constant phase $\varphi_m(L_e)$, the first order term is the angle correction $\delta\theta_{est}(L_e)$ and the second order term can be used to compute the distance to the source $R_{est}(L_e)$ (see §3.3). We then take the mean value of the two L_e, denoted $\delta\theta_{est}$ and R_{est} and use them to correct the filter as in (25). This choice $L \sim \frac{L_{kr_0}}{2}$ appears as a compromise (L large/small) and the averaging process is only due to an observation that the results improve (slightly) when we use it.

We thus obtain a new corrected value sequence β_q. Assuming the maximum in modulus is reached for $q = q\star$, the angle $\theta_{est} = \frac{2\pi(q^\star-1)}{Q} + \delta\theta_{est}$ is the new approximation of the incidence angle while $\beta_{q^\star}$ approximated the asymptotic amplitude of the source point data

$$\beta_{q^\star} = B_{est}(k) \simeq B_{exact} = \frac{e^{ikR}}{\sqrt{-8i\pi R}}.$$

We present below numerical results comparing this algorithm using `NMLA` and its Gaussian weight version of §5 where we use $\tau = \sqrt{\frac{2}{7}}$.

6.3. Numerical results

6.3.1. For fixed k We fix the wavelength to 2.5 centimeters or $kR = 40\pi \simeq 251.32..$ Using the law found in §6.2 the radius of the observation circle is

$$r_0 \simeq 14.46 \text{ cm}.$$

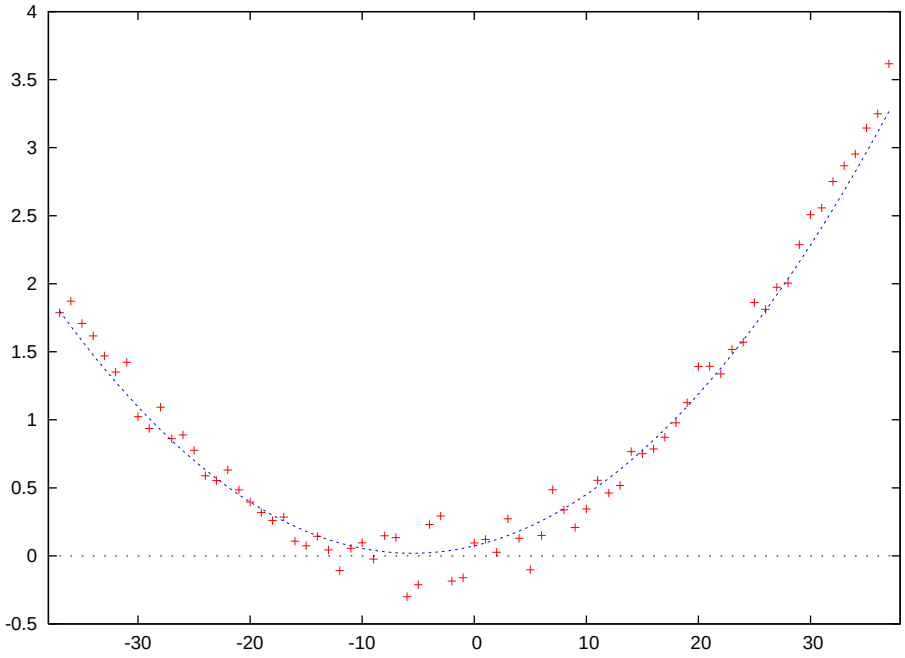

Figure 2. $\ell \mapsto \varphi_\ell$ (crosses) and parabolic fitting (dashed curve)

The grid noise in relative L^2 norm with $h = \frac{\lambda}{10}$ is 22%. We apply B_k^P and its Gaussian weight version ($L_{kr_0} = 37$) to this data. In Figure 3 we plot β_p the output of the filter versus the angle in degrees. The left column is the first `NMLA` pass, the right is the curvature correction (second `NMLA`) pass. The top row corresponds to the regular `NMLA` filter, the bottom row the Gaussian weight version.

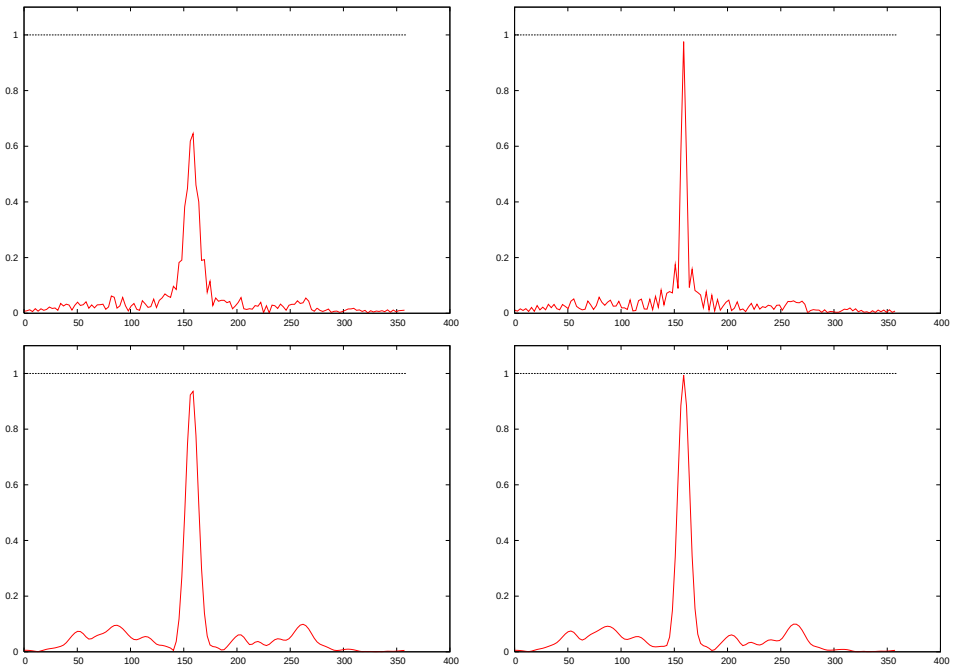

Figure 3. θ (in degree) $\mapsto \frac{|\beta(\theta)|}{|B_{exact}|}$. Left column first `NMLA` pass, right column second `NMLA` pass (curvature correction). Top row: standard filter; Bottom row : Gaussian weight filter.

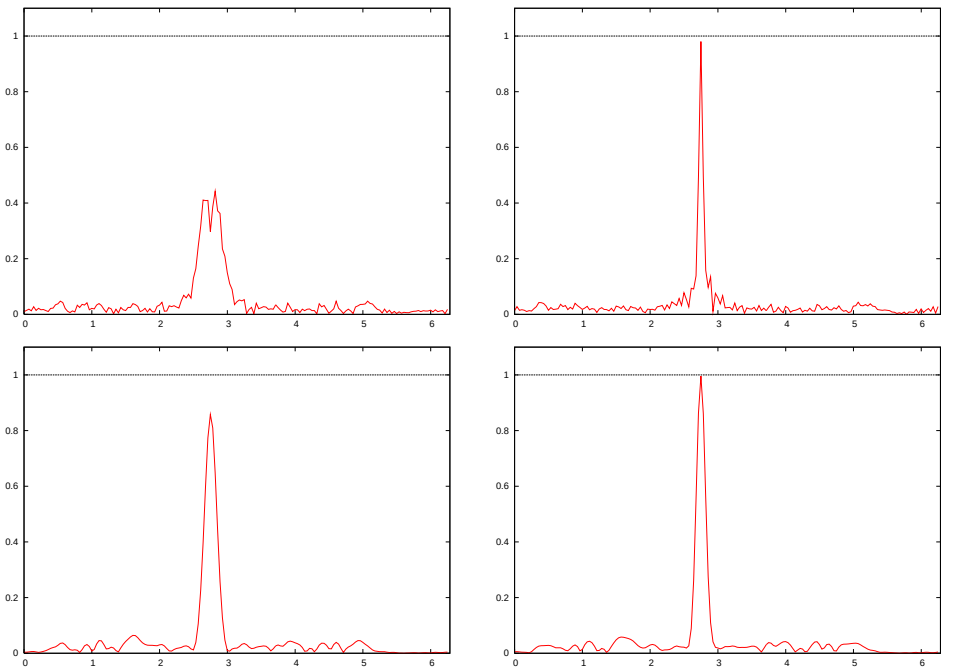

Figure 4. Same as figure 3 but with $R_{-} = 1.1 R_{exact}$.

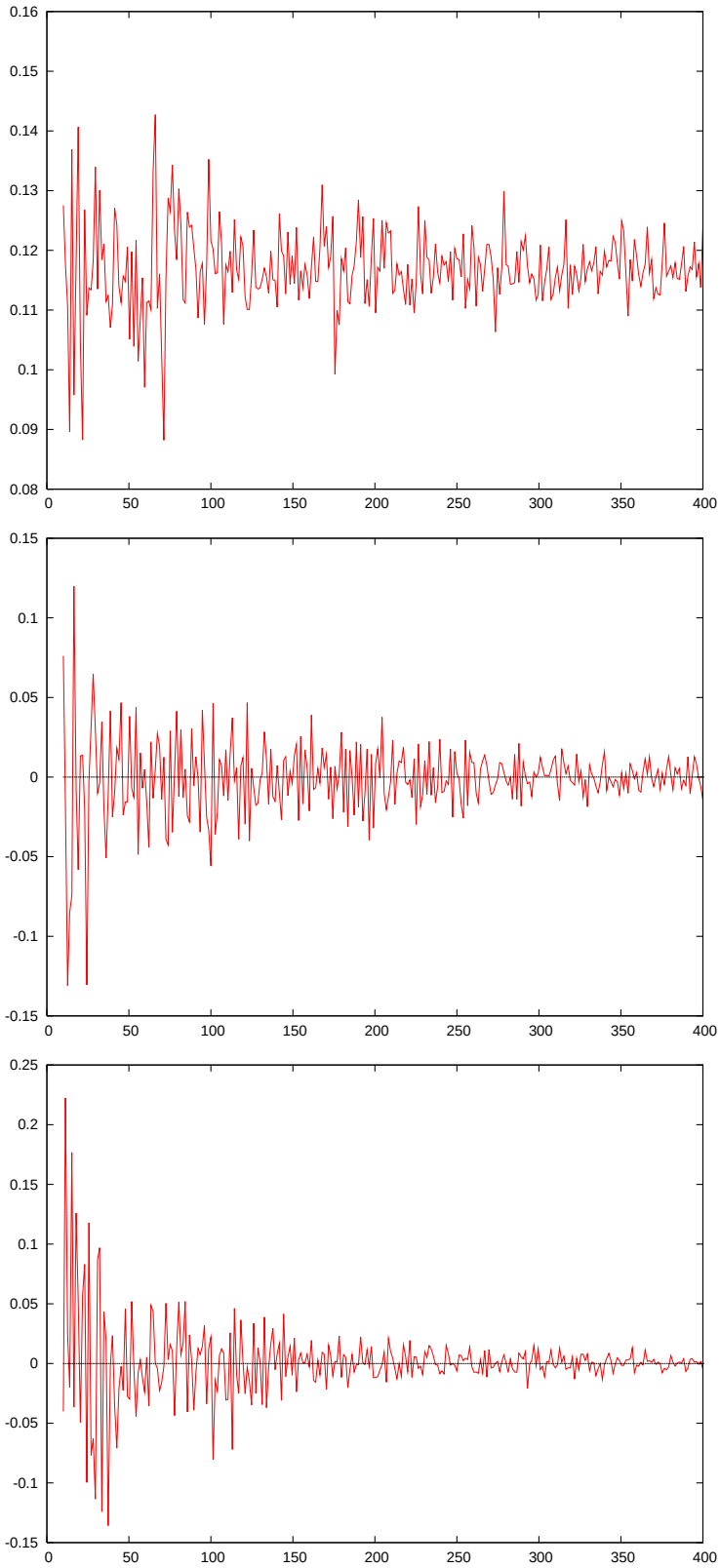

Figure 5. Top : $\frac{k}{2\pi} \mapsto \frac{|U_{noisy}(k)|_{L^2(R)} - |U_{exact}(k)|_{L^2(R)}}{|U_{exact}(k)|_{L^2(R)}}$. Middle : $\frac{k}{2\pi} \mapsto \frac{|R_{est}(k)| - R|}{R}$. Bottom : $\frac{k}{2\pi} \mapsto \theta_i - \theta_{est}(k)$.

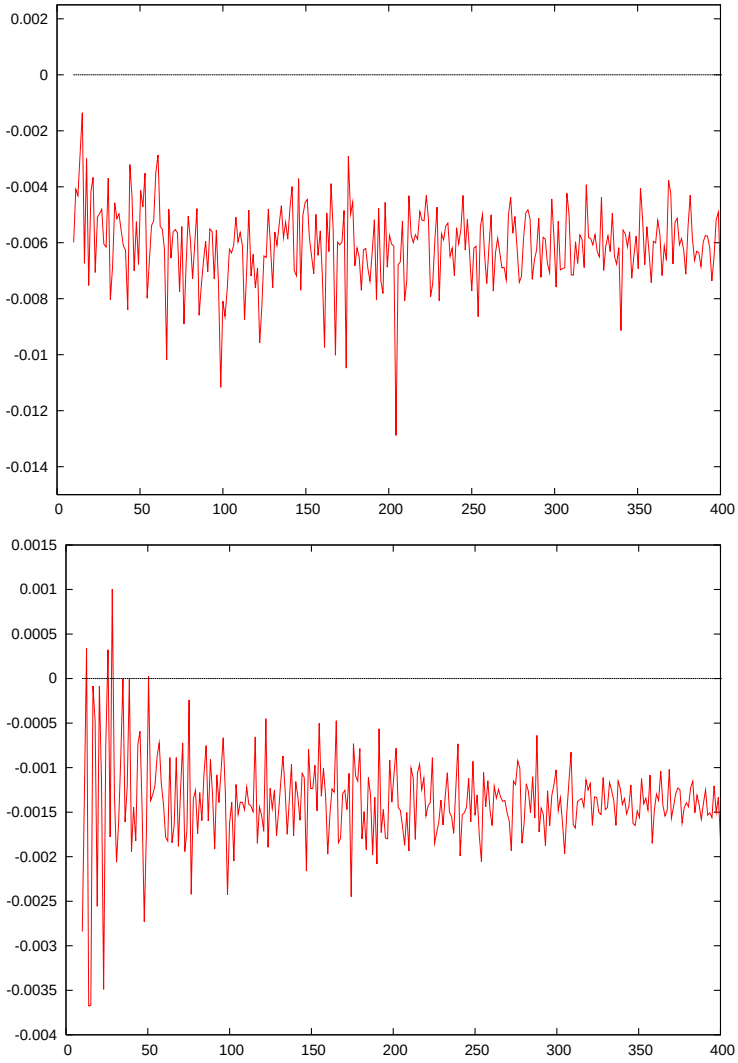

Figure 6. $\frac{k}{2\pi} \mapsto \frac{|B_{est}(k)|-|B_{exact}|}{|B_{exact}|}$. Top : standard `NMLA`. Bottom : Gaussian weight version.

We notice that all filters peaks are located near the correct angle. Amplitude and angles are not very accurate for the first pass (especially for the non Gaussian weight version) because the plane wave approximation error is too large for this r_0 (81% in relative L^2 norm). The maximum is reached at $\theta_i + 1.05$ degree.

The parabolic fit of (24) is presented in figure 2; we indeed observe a cloud of points around a parabola. The estimated curvature is $R_{est} = 1.1075$ meter (10% error).

The curvature correction (second pass) on the right is sharper. We get

$$\theta_{est} - \theta_i = -0.037\text{degree}, \quad \frac{|B_{est}| - |B_{exact}|}{|B_{exact}|} \simeq -2.2\%,$$

while for the Gaussian filter,

$$\theta_{est} - \theta_i = -0.037\text{degree}, \quad \frac{|B_{est}| - |B_{exact}|}{|B_{exact}|} \simeq -0.5\%.$$

We remark that the Gaussian weight version (bottom) does a better job on the modulus of the amplitude.

One can improve this result by running the algorithm §6.2 again but with the better estimate we just found for R : $R_{-} = 1.10075$ meter. The result is shown in figure 4. The radius r_0 is then larger ($24.7cm$) and the new estimated curvature R_{est} is found to be 1.01 meter (1% error).

6.3.2. Varying k We study numerically the result of algorithm §6.2 when k takes 300 values such that the source-observation distance $R = 1$ represents between 10 and 400 wavelengths.

The "noise" grid step is one tenth of the wavelength. The relative noise level on the data varies with k between 8 and 14% (See figure 5, top).

The curvature estimate $R_{est}(k)$ varies around the exact value $R = 1$ with an error which decreases with k down to 2% from a maximum at 10% (cf. figure 5, middle). The error on the angle (Figure 5 bottom) shows a maximum of 0.2 degree but then decreases to 0.01 degree for high frequencies.

There are no noticeable differences when we use the Gaussian weight filter except on the modulus of the amplitude. Figure 6 shows the relative error for this quantity which is underestimated by 0.8% for the standard `NMLA` (top) and 0.15% for the Gaussian weight filter (bottom).

References

[1] Jean-David Benamou, Francis Collino, and Simon Marmorat. Source point discovery through high frequency asymptotic time reversal. *Journal of Computational Physics, to appear.*

[2] Jean-David Benamou, Francis Collino, and Olof Runborg. Numerical microlocal analysis of harmonic wavefields. *J. Comput. Phys.*, 199(2):717–741, 2004.

[3] Gregory Beylkin. Discrete Radon transform. *IEEE Trans. Acoust. Speech Signal Process.*, 35(2):162–172, 1987.

[4] D. Bouche, F. Molinet, and R. Mittra. *Asymptotic methods in electromagnetics.* Springer-Verlag, Berlin, 1997. Translated from the 1994 French original by Patricia and Daniel Gogny and revised by the authors.

[5] Q. Carayol and F. Collino. Error estimates in the fast multipole method for scattering problems. II. Truncation of the Gegenbauer series. *M2AN Math. Model. Numer. Anal.*, 39(1):183–221, 2005.

[6] Quentin Carayol and Francis Collino. Error estimates in the fast multipole method for scattering problems. I. Truncation of the Jacobi-Anger series. *M2AN Math. Model. Numer. Anal.*, 38(2):371–394, 2004.

[7] V. Červený. *Seismic ray theory*. Cambridge University Press, Cambridge, 2001.

[8] T.M. Cherry. Uniform asymptotic formulae for functions with transition points. *Trans. AMS*, 68:224–257, 1950.

[9] F. Collino. Conditions aux limites absorbantes d'ordre élevé pour les modèles de propagation d'onde. problème des domaines rectangulaires. Technical Report 1790, INRIA., Domaine de Voluceau, Rocquencourt, France, 1992.

[10] D. Colton and R. Kress. *Inverse Acoustic and Electromagnetic Scattering Theory*, volume 93. Springer-Verlag, 1992.

[11] M. V. Fedoryuk. *Partial differential equations. V*, volume 34 of *Encyclopaedia of Mathematical Sciences*. Springer-Verlag, Berlin, 1999. Asymptotic methods for partial differential equations, A translation of ıt Current problems in mathematics. Fundamental directions. Vol. 34 (Russian), Akad. Nauk SSSR, Vsesoyuz. Inst. Nauchn. i Tekhn. Inform., Moscow, 1988 [MR1066954 (91e:35002)], Translation by J. S. Joel and S. A. Wolf, Translation edited by M. V. Fedoryuk.

[12] S. Fomel. Applications of plane-wave destructor filters:. Technical Report 105, SEP, 2000.

[13] Yanina Landa, Nicolay M. Tanushev, and Richard Tsai. Discovery of point sources in the Helmholtz equation posed in unknown domains with obstacles. *Commun. Math. Sci.*, 9(3):903–928, 2011.

[14] B. Porat and B. Friedlander. Analysis of the asymptotic relative efficiency of music algorithm. *IEEE Trans. Acoust., Speech Signal Process.*, 36(4):532–544, 1988.

[15] G. N. Watson. *A treatise on the theory of Bessel functions*. Cambridge University Press, 1966.

Appendix A. Uniform estimate in k of the filter norm

The definition of the filter (4) introduces a truncation integer L_{kr_0}, $L_{kr_0} = L^\star(kr_0)$ with

$$L^\star(x) = \max\left(1, [x], [x + x^{\frac{1}{3}} - 2.5]\right). \tag{A.1}$$

The particular choice of $L^\star$ arises from two opposing conditions on L_{kr_0} :

First, the larger the truncation integer the better the accuracy of the angle extraction process (see section 2).

Second, we want the norm of the filter operator to be small in order to control the effect of the noise. We established in §2.1, inequality (8), that the norm of the filter is bounded by $N(L_{kr_0}, kr_0)$, the square of $N(L, x)$ defined as

$$N^2(L, x) = \frac{1}{(2L+1)^2} \sum_{n=-L}^{L} \frac{1}{J_n^2(x) + J_n'^2(x)}. \tag{A.2}$$

We prove below that $L \mapsto N(L, x)$ goes to infinity with L. This implies that we need to introduce an upper bound on L_{kr_0}.

This appendix shows that it is possible to control $N(L(x), x)$ uniformly on x for some $L(x)$ that grows like x when x is large.

Appendix A.1. Numerical behavior of the filter norm

We begin with a numerical estimation of $N(L, x)$ and of the optimal mode truncation law $L^*(x)$.

First, this function is well defined since $J_n(x)$ and $J_n'(x)$ have no common zeros. This is due to the Wronksian formula for Bessel functions, [15, pp 76],

$$J_n(x)Y_n'(x) - J_n'(x)Y_n(x) = \frac{2}{\pi x}, \tag{A.3}$$

where $Y_n(x)$ is the *Neumann Function*, see [15, pp 64].

A straightforward calculation gives $N^2(1, 0) = 1$ and, due to the *Hansen Equality* and its variant,

$$\sum_{n=-\infty}^{\infty} J_n^2(x) = 1, \quad \sum_{n=-\infty}^{\infty} J_n'^2(x) = \frac{1}{2},$$

Cauchy-Schwarz inequality provides $N^2(L, x) > \frac{2}{3}$. Now, let us look at the curves $L \mapsto N(L, x)$ for different positive values of x: Figure A1 shows that this sequence is at first decreasing on some interval $[1, L_{opt}(x)]$ then increasing for L in $[L_{opt}(x), +\infty[$, the increasing rate being more than exponential when L overpasses a value slightly larger than x. In Figure A2, we show the numerical behavior of functions $x \mapsto N(L, x)$ for different values of L; it appears that the minimum over all L of $N(L, x)$ remains between 0.8 and 1. It is possible to approximate numerically the integer $L^{opt}(x)$ (i.e. the integer which provides the minimum of $N(L, x)$ for a given x): for x large enough (> 5) and less than 8000 we find

$$L^{opt}(x) \simeq x + x^{\frac{1}{3}} - 2.5.$$

We infer that $B^\star = \max_x N(L^\star(x), x)\ L^\star(x)$ defined in (A.1) should remain finite and closed to the "optimal value" $\max_x N(L^{opt}(x), x)$, whence the choice $L_{kr_0}(r_0) = L^\star(kr_0)$ in the definition of the filter.

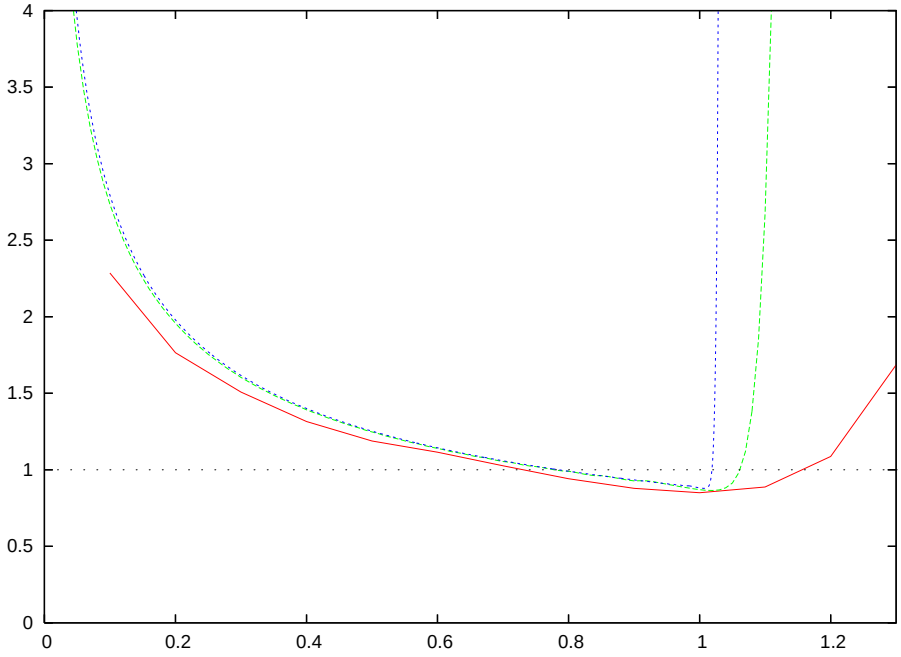

Figure A1. Sequence $L \mapsto N(L, x)$ for $x = 10$ (red), 100 (green), 1000 (blue). Horizontal axis is $\frac{L}{x}$.

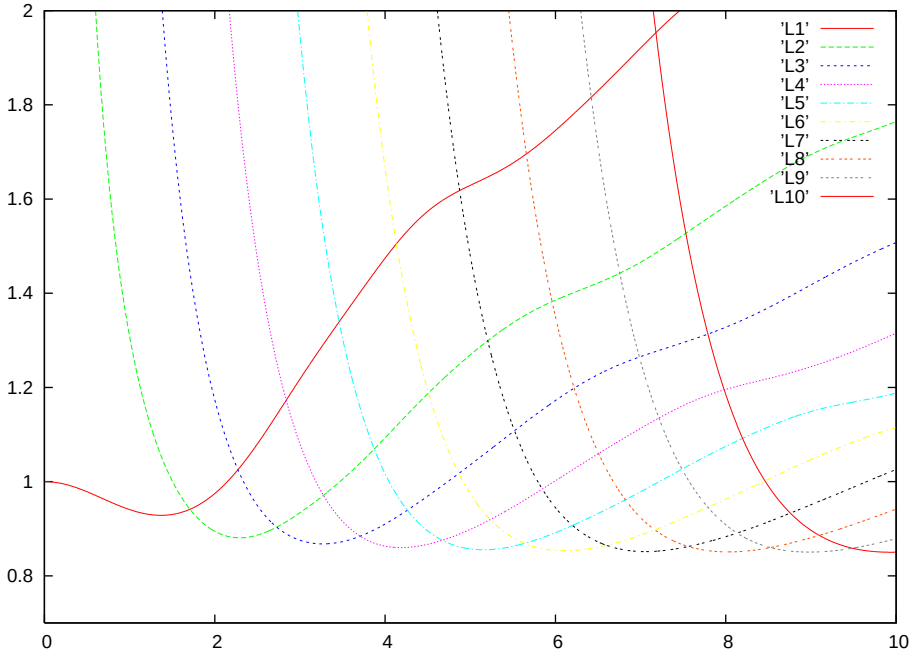

Figure A2. Functions $x \mapsto N(L, x)$ for $L = 1, \ldots 10$. For each x the lowest $N(L, x))$ can be read as the lowest envelop of all the curves.

Remark Long technical arguments we skipped here, give evidence that a better

approximation of $L^{opt}(x)$ is

$$L^{opt}(x) \simeq \max(1, x + \left[\frac{1}{32} W^2\left(\frac{x}{4}\left(\frac{8}{3\pi}\right)^3\right)\right]^{\frac{1}{3}} x^{\frac{1}{3}}),$$

where $u \mapsto W(u)$ is the Lambert function, see (32).

Appendix A.2. The stability result

We prove the

Theorem 1 *There exists pure constants, $B^\star$ and C such that*

$$\max_{x\geq 0} N^2(L^\star(x), x) = (B^\star)^2 \tag{A.4}$$

$$\text{and} \quad \sup_{\left\{(L,x)/0\leq x\leq L\leq x+x^{\frac{1}{3}}\right\}} N^2(L,x) \leq C, \tag{A.5}$$

with $N(L,x)$, $L^\star(x)$ defined in (A.2), (A.1) respectively.

Proof : We remark that, $(L^\star(x), x)$ is always in $\mathcal{S} = \left\{(L,x)/0 \leq x \leq L \leq x + x^{\frac{1}{3}}\right\}$; it implies that (A.4) with $B^\star < \sqrt{C}$ is a direct consequence of (A.5). it is therefore enough to establish (A.5). As a preamble, we recall that since $J_{-n}(x) = (-1)^n J_n(x)$, see [15, (2) page 15], we have as well

$$N^2(L,x) = \frac{1}{(2L+1)^2} \sum_{n=0}^{L} \varepsilon_n \frac{1}{J_n^2(x) + J_n'^2(x)},$$

where $\varepsilon_0 = 1$, and $\varepsilon_n = 2$ when $n \neq 0$. Thus, we can work with Bessel functions of non negative order.

For technical reasons, we consider separately the cases x "small" and x "large". More precisely, let x_0 be large enough to satisfy

$$x + x^{\frac{1}{3}} - x^{\frac{2}{3}} + 1 \leq \sqrt{x^2 - 1}, \text{ for all } x > x_0. \tag{A.6}$$

Numerically, we find $x_0 = 4.6237...$

First, we consider the case $x < x_0$; the function $x \mapsto (x + \frac{1}{2})(J_n^2(x) + J_n'^2(x))$ is non negative and does not vanish for $x > 0$. Moreover, it tends to $\frac{2}{\pi}$ when x goes to infinity since, cf. [15, page 199]

$$J_n(x) = \sqrt{\frac{2}{\pi x}} \cos\left(x - \frac{\pi}{2}(n + \frac{1}{2})\right)\left(1 + O(x^{-1})\right),$$

$$J_n'(x) = \frac{1}{2}\left(J_{n-1}(x) - J_{n+1}(x)\right) = \sqrt{\frac{2}{\pi x}} \sin\left(x - \frac{\pi}{2}(n + \frac{1}{2})\right)\left(1 + O(x^{-1})\right).$$

We deduce that there are some constants β_n such that

$$\frac{1}{(x + \frac{1}{2})(J_n^2(x) + J_n'^2(x))} \leq \beta_n,$$

and, consequently

$$N^2(L,x) \leq \frac{x + \frac{1}{2}}{(2L+1)^2} \sum_{n=0}^{L} \varepsilon_n \beta_n.$$

Now, as $x < x_0$, we have if $L \leq [x + x^{\frac{1}{3}}] \leq [x_0 + x_0^{\frac{1}{3}}]$,

$$N^2(L,x) \leq \frac{x_0 + \frac{1}{2}}{[2 \times 0 + 1]^2} \sum_{n=0}^{[x_0 + x_0^{\frac{1}{3}}]+1} \varepsilon_n \beta_n = C^{ste}.$$

If the norm $N^2(L,x)$ diverged over $x \leq L \leq x + x^{\frac{1}{3}}$, it could only be for x large.

Consider now x large, i.e. $x > x_0$. Bounding above being easier than bounding below, we use the identity

$$\frac{1}{J_n^2(x) + J_n'^2(x)} = \frac{Y_n^2(x) + Y_n'^2(x)}{(J_n(x)Y_n(x) + J_n'(x)Y_n'(x))^2 + (J_n(x)Y_n'(x) - J_n'(x)Y_n(x))^2}.$$

We recognize in the second term inside the denominator the square of the Wronksian (A.3); we then have

$$\frac{1}{J_n^2(x) + J_n'^2(x)} \leq \frac{\pi^2 x^2}{4} \left(Y_n^2(x) + Y_n'^2(x) \right).$$

To get rid of the derivative, we use

$$Y_n'(x) = \frac{1}{2} \left(Y_{n-1}(x) - Y_{n+1}(x) \right), \; n \neq 0, \quad Y_0'(x) = -Y_1(x)$$

and therefore

$$\frac{1}{J_n^2(x) + J_n'^2(x)} \leq \frac{\pi^2 x^2}{4} \left(Y_n^2(x) + \frac{1}{2} Y_{n-1}^2(x) + \frac{1}{2} Y_{n+1}^2(x) \right),$$

from which, we deduce (the constant π^2 is not optimal)

$$N^2(L,x) \leq \pi^2 \frac{x^2}{(2L+1)^2} \sum_{n=0}^{L+1} Y_n^2(x) \tag{A.7}$$

We are going bound above the right hand side of (A.7). We split the summation over n into four parts: $n = 0$, then $n = 1, \ldots Q$, then $n = Q+1, \ldots L-1$ and at finally $n = L, L+1$ where Q is chosen such that

$$x + x^{\frac{1}{3}} - x^{\frac{2}{3}} \leq Q < \sqrt{x^2 - 1}.$$

Such an integer does exist since the difference between the upper and lower bounds is always larger than 1 when $x > x_0$ (x_0 was precisely chosen for that). In the following, we will often use the square of the modulus of the Hankel function $J_n(x) + iY_n(x)$ since one controls rather well its behavior, thanks to the *Nicholson formula*, [15, page 444]

$$J_n^2(x) + Y_n^2(x) = \frac{8}{\pi} \int_0^\infty K_0(2x \sinh t) \cosh(2nt)\, dt,$$

where $K_0(u) = \int_0^\infty e^{-u \cosh \xi}\, d\xi$ is the *Kelvin function*.

(i) For $n = 0$: as $x \mapsto J_n^2(x) + Y_n^2(x)$ is a decreasing function, [15, page 446]. So, for $x \in [x_0, ; \infty]$

$$Y_0^2(x) \leq J_0^2(x_0) + Y_0^2(x_0) = C_0. \tag{A.8}$$

(ii) For $n = 1, \dots Q$: we use [15, page 447], when $x \geq n \geq \frac{1}{2}$

$$J_n^2(x) + Y_n^2(x) \leq \frac{2}{\pi} \frac{1}{\sqrt{x^2 - n^2}},$$

and therefore

$$\sum_{n=1}^{Q} Y_n^2(x) \leq \frac{2}{\pi} \sum_{n=1}^{Q} \frac{1}{\sqrt{x^2 - n^2}},$$

but, since the sequence $n \mapsto \frac{1}{\sqrt{x^2-n^2}}$ is increasing, we have

$$\sum_{n=1}^{Q} J_n^2(x) + Y_n^2(x) \leq \frac{2}{\pi} \left(\frac{1}{\sqrt{x^2 - Q^2}} + \int_0^Q \frac{d\nu}{\sqrt{x^2 - \nu^2}} \right),$$

or

$$\sum_{n=1}^{Q} J_n^2(x) + Y_n^2(x) \leq \frac{2}{\pi} \left(\frac{1}{\sqrt{x^2 - Q^2}} + \left[\arcsin \frac{\nu}{x} \right]_{\nu=0}^{Q} \right) \leq \frac{2}{\pi} \left(\frac{1}{\sqrt{x^2 - Q^2}} + \pi \right).$$

Now, we recall that the Q was chosen such that $Q \leq \sqrt{x^2 - 1}$ and therefore $\frac{1}{\sqrt{x^2-Q^2}} \leq 1$; we deduce

$$\sum_{n=1}^{Q} J_n^2(x) + Y_n^2(x) \leq \frac{2}{\pi}(1 + \pi) = C_1. \tag{A.9}$$

(iii) For $n = Q + 1, \dots L - 1$: function $\nu \mapsto J_\nu^2(x) + Y_\nu^2(x)$ is increasing (cf. Nicholson formula), we thus have

$$\sum_{n=Q+1}^{L-1} Y_n^2(x) \leq \sum_{n=Q+1}^{L-1} J_n^2(x) + Y_n^2(x) \leq (L - Q) \left(J_{L-1}^2(x) + Y_{L-1}^2(x) \right).$$

But if $L \leq x + x^{\frac{1}{3}} + 1$, we have

$$\sum_{n=Q+1}^{L-1} J_n^2(x) + Y_n^2(x) \leq (L - Q) \left(J^2_{x+x^{\frac{1}{3}}}(x) + Y^2_{x+x^{\frac{1}{3}}}(x) \right) = (L - Q)\Psi(x).$$

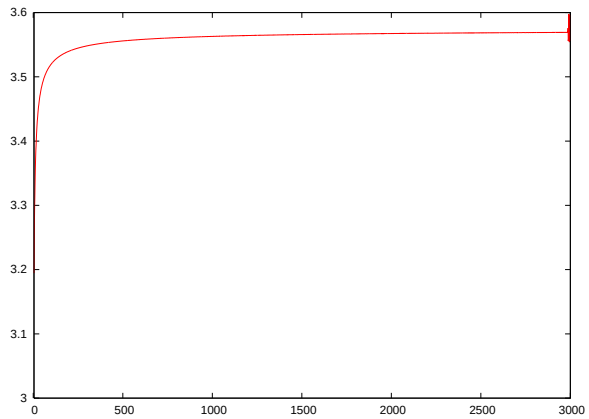

Figure A3. Graph of Function $x^{\frac{2}{3}}\Psi(x)$ over $x \in [4, 3000]$

The behavior of function $\Psi(x)$ for x large can be deduced from the approximations of Bessel's Functions $J_n(x)$, $Y_n(x)$ with $n \sim x$. From the estimates given in [8], we deduce (painfully) that when κ is given and x is large,

$$J_{x+\kappa x^{\frac{1}{3}}}(x) \simeq \left(\frac{2}{x}\right)^{\frac{1}{3}} \mathrm{Ai}(2^{\frac{1}{3}}\kappa), \quad Y_{x+\kappa x^{\frac{1}{3}}}(x) \simeq -\left(\frac{2}{x}\right)^{\frac{1}{3}} \mathrm{Bi}(2^{\frac{1}{3}}\kappa),$$

Where Functions Ai and Bi are the *Airy Functions* . Thus (cf. Fig A3), there exists a constant C_2 such that

$$\sup_{x>x_0} x^{\frac{2}{3}} \left(J^2_{x+x^{\frac{1}{3}}}(x) + Y^2_{x+x^{\frac{1}{3}}}(x)\right) \leq C_2,$$

and therefore

$$\sum_{n=Q+1}^{L-1} J_n^2(x) + Y_n^2(x) \leq \frac{(L-Q)}{x^{\frac{2}{3}}} C_2 \leq C_2, \tag{A.10}$$

The last equality coming from the bound

$$L - Q \leq x + x^{\frac{1}{3}} - (x + x^{\frac{1}{3}} - x^{\frac{2}{3}}) = x^{\frac{2}{3}}.$$

(iv) For the two last terms of the series L, $L+1$: in order to use the previous estimate, we move back twice on the order of the Bessel functions . Since

$$Y_{n+1}(x) = -Y_{n-1}(x) + \frac{2n}{x} Y_n(x),$$

we have

$$\frac{1}{2} Y^2_{n+1}(x) \leq Y^2_{n-1}(x) + \frac{4n^2}{x^2} Y_n^2(x),$$

and, by successive bounding, we get

$$Y_n^2(x) + Y^2_{n+1}(x) \leq 2\left(1 + \frac{8n^2}{x^2}\left(1 + \frac{4(n-1)^2}{x^2}\right)\right) \max\left(Y^2_{n-2}(x), Y^2_{n-1}(x)\right).$$

and therefore

$$Y_n^2(x) + Y^2_{n+1}(x) \leq 2\left(1 + \frac{8n^2}{x^2}\left(1 + \frac{4n^2}{x^2}\right)\right) \left(Y^2_{n-1}(x) + J^2_{n-1}(x)\right)$$

and that, always thanks to the increasing property of the sequence $n \mapsto J_n^2(x) + Y_n^2(x)$. We are brought to the previous bound. Thus, we have, when $L < x + x^{\frac{1}{3}}$

$$\sum_{n=L}^{L+1} Y_n^2(x) \leq 2\left(1 + \frac{8L^2}{x^2}\left(1 + \frac{4L^2}{x^2}\right)\right) (J^2_{x+x^{\frac{1}{3}}}(x) + Y^2_{x+x^{\frac{1}{3}}}(x)),$$

or also, when $x_0 \leq x \leq L \leq x + x^{\frac{1}{3}}$,

$$\sum_{n=L}^{L+1} Y_n^2(x) \leq 2\left(1 + \frac{8(x+x^{\frac{1}{3}})^2}{x^2}\left(1 + \frac{4(x+x^{\frac{1}{3}})^2}{x^2}\right)\right) \frac{C_2}{x^{\frac{2}{3}}} \leq C_3. \tag{A.11}$$

We gather all our results, when $x + x^{\frac{1}{3}} > L > x > x_0$, there exists four constants such that

$$N^2(L,x) \leq \pi^2 \frac{x^2}{(2L+1)^2} (C_0 + C_1 + C_2 + C_3) \leq \pi^2 (C_0 + C_1 + C_2 + C_3),$$

and since $N^2(L,x)$ is uniformly bounded over $x \leq x_0$ and $L \leq [x_0 + x_0^{\frac{1}{3}}]$, the proof is complete. □